2014 IEEE/RSJ International Conference on
Intelligent Robots and Systems (IROS 2014)
September 14-18, 2014, Chicago, IL, USA

Toward a Modular Soft Sensor-Embedded Glove for Human Hand Motion and Tactile Pressure Measurement

Frank L. Hammond III, *Member, IEEE,* Yiğit Mengüç, *Member, IEEE* and Robert J. Wood, *Member, IEEE*

***Abstract*—The ability to measure human hand motions and interaction forces is critical to improving our understanding of manual gesturing and grasp mechanics. This knowledge serves as a basis for developing better tools for human skill training and rehabilitation, exploring more effective methods of designing and controlling robotic hands, and creating more sophisticated human-computer interaction devices which use complex hand motions as control inputs. This paper presents work on the design, fabrication, and experimental validation of a soft sensor-embedded glove which measures both hand motion and contact pressures during human gesturing and manipulation tasks. We design an array of liquid-metal embedded elastomer sensors to measure up to hundreds of Newtons of interaction forces across the human palm during manipulation tasks and to measure skin strains across phalangeal and carpal joints for joint motion tracking. The elastomeric sensors provide the mechanical compliance necessary to accommodate anatomical variations and permit a normal range of hand motion. We explore methods of assembling this soft sensor glove from modular, individually fabricated pressure and strain sensors and develop design guidelines for their mechanical integration. Experimental validation of a soft finger glove prototype demonstrates the sensitivity range of the designed sensors and the mechanical robustness of the proposed assembly method, and provides a basis for the production of a complete soft sensor glove from inexpensive modular sensor components.**

I. Introduction

Experimental measurement and characterization of human hand mechanics are critical to many active areas of academic research and commercial product development, including the design of robotic hands and teleoperative robotic instruments, the development of consumer devices such as input devices for the control of robots, virtual reality-based design interfaces [1], arts and entertainment [2], and information manipulation and communication, and the design of diagnostic medical devices such as wearable hand rehabilitation and patient monitoring systems [3]. A majority of the solutions designed for human motion tracking and grasp force measurement are wearable glove-based devices [4,5] (Fig. 1). These devices vary widely in core sensing technologies, device complexity, data richness (resolution, bandwidth), and mechanical robustness, some of which are dictated by target application requirements.

Manuscript received February 6, 2014, final paper submitted on June 21, 2014. F. L. Hammond III, Y. Mengüç and R. J. Wood are with the Harvard School of Engineering and Applied Sciences, 60 Oxford Street, Cambridge, MA 02138 USA (email: fhammond@seas.harvard.edu).

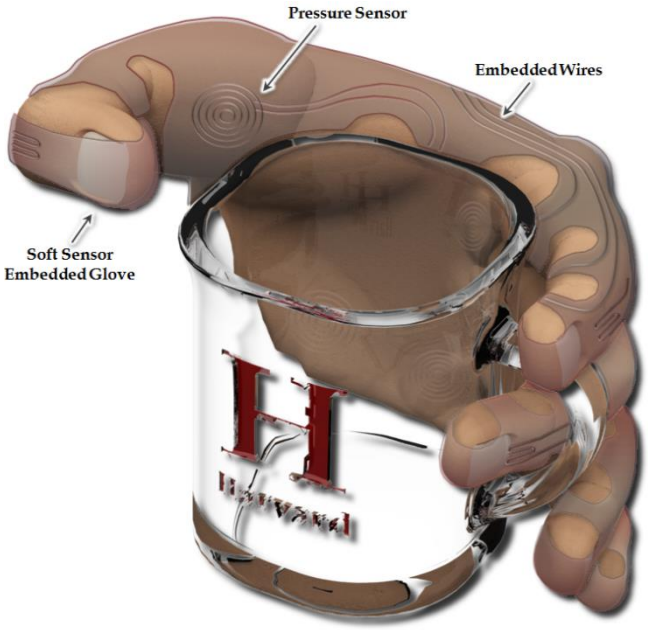

Fig. 1. Concept drawing the proposed soft sensor glove with integrated force and strain sensors responding to joint motion and finger pad contact.

Early devices such as the Data Glove [4,5] and Space Glove [5] used fiberoptic tubes to measure curvature across individual finger joints (15 joints for the Data Glove). More recent devices such as the CyberGlove [5], Super Glove [4], and several research-grade devices [2,6] use piezoresistive elements to measure several hand degrees of freedom (22 DOFs for CyberGlove). Devices like the Accele Glove [8] and KHU-1 glove [8] use networks of accelerometers and inertial measurement units (IMUs) to track fingertip positions. Other devices use visual motion data [9], optical sensing [10], and electromagnetic trackers to record complex hand motions, and a few also use piezoresistive films to detect tactile pressures (FingerTPS, PPS Inc.). These glove-based measurement systems have demonstrated the ability to track many degrees of hand motion precisely, but the complexity and cost of fabrication (sensor integration), signal processing requirements (noisy sensors), and packaging and assembly limitations have made these particular devices economically prohibitive to manufacture and difficult to use during every day activities. More importantly, most devices lack force/pressure measurement capabilities critical to grasp mechanics research and the development of better human-computer interaction devices.

The availability of inexpensive, compliant polymers and electrically conductive liquids and gels has made the design and manufacturing of multimodal sensing gloves more tractable, both in economy and in the feasibility of engineering and integrating sensing components. Several recent data glove devices have made use of these materials, including gloves with conductive polymers printed onto flexible substrates for joint sensing [11], fabric gloves with embedded conductive polymer strain sensors [12], conductive liquid embedded elastomeric sensors [13], and stereolithographic printing of monolithic gloves with photopolymers and conductive gels [14]. These devices have the advantages of being inexpensive, having flexibility of design (capability limited only by printing and modeling methods), and being intrinsically compliant such that they accommodate anatomical variations. However, current soft sensor manufacturing methods are not yet mature enough to allow repeatable, high-yield production of complicated soft sensor networks required for multi-DOF wearable devices.

This paper describes the design and validation of a low-profile, modular, soft sensor-embedded glove which - unlike most previous data gloves - measures both human hand motions and tactile pressures. We demonstrate new mechanical integration methods which permit both modular fabrication of soft sensors and their assembly into such soft networks for wearable devices, and we detail enabling process innovations such as wire embedding and encapsulation molds. Novel soft sensor fabrication methods described in [15-16] are leveraged to create the soft pressure and tensile strain sensors which we integrate with our assembly method. The result is an inexpensive, easy to manufacture data glove which adapts to anatomical variations and measures the motions of all finger joints and the pressures major contact surfaces on the hand, providing a rich data set. Target applications of this novel glove include:

- *Study of Human Grasp Mechanics*: measuring joint motion and contact pressures as humans manipulate daily living objects is important to development of robotic hands, hand prostheses, and grasp-assist devices. Reliable data of this sort does not yet exist.
- *Skill Training and Rehabilitation*: the glove can be used to train a person for a certain manual skill by providing real-time feedback on contextual motion quality.
- *Gaming and Telepresence*: consumer entertainment and productivity applications where hand gesturing can be used to control devices and virtual objects.

Section II describes the glove performance requirements derived from human anatomical and biomechanics data. Section III describes soft sensor design and evaluation efforts, and Section IV outlines the fabrication process. Section V presents preliminary experiments done using a "soft finger glove" prototype. Section VI discusses the results of those tests and provides insights from experiments. Section VII outlines future work on soft sensor glove design.

II. Performance Requirements

The proposed soft sensor-embedded glove has several performance requirements derived from knowledge of human anatomy and anatomical variation [23] (ensuring comfort and proper sensor location) and from experimental characterization of human grasp mechanics and interaction forces (tuning sensors to measure expected forces and motions). In our design process, we consider degrees of freedom (Section II-A), maximal grasping forces (Section II-B), and anatomical variations of the human hand (Section II-C) in selecting these performance requirements.

A. Degrees of Freedom and Motion Ranges

The topology of the proposed soft sensor glove is based loosely on a human hand model which has 24 kinematic DOFs [17] (Fig. 2). To simplify the soft glove design and minimize the number of sensors needed, we focus only those joints that contribute to gross finger motions during object grasping and manipulation. We aim to measure finger and thumb motion relative to the wrist reference frame, so the CMC joints - which contribute primarily to wrist articulation – are not considered for this instantiation of the human hand model. This reduces the kinematic DOFs and, by extension, the number of joint motion sensors in the data glove to 20.

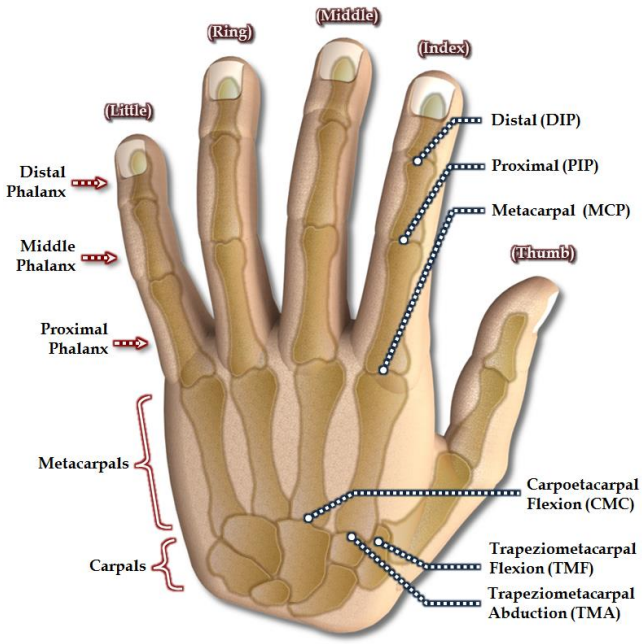

Fig. 2. The skeletal anatomy of the human hand with joint locations.

The abduction-adduction motions of the fingers and thumb are measured here as motion differences or angles between fingers (inter-digital abduction, or IDA) rather than as individual motions, further reducing our hand model to 19 DOFs. We specify the motion ranges for each of these 19 DOFs in our reduced model according to experimental characterizations of hand motion found in [18] and use these as motion range targets for the glove (Table 1).

TABLE I
HUMAN HAND DEGREES OF FREEDOM AND MOTION RANGES (°)

Digit \ Joint	*TPF*	*IDA/TPA*	*MCP*	*PIP*	*DIP*
Thumb	0-50	**30**-70	0-55	5-90	NA
Fingers	NA	0-60	**45**-90	0-115	**20**-90

Bold numbers indicate joint hyperextension beyond the 0° neutral position. Trapeziometacarpal flexion (TPF) is measured with respect to a flat palm hand posture where larger angle values indicate greater proximity of the thumb base to the palm.

B. Grasping Forces and Human Proprioception

Previous research on human grasping capabilities [19] demonstrated that the human hand can exert as much force as 450N in males and 350N in females. The distribution of these forces over the volar surface (the palm) of the hand can vary according to the shape of the object being grasped, producing pressure concentrations in certain areas. Rather than defining the maximum expected pressure as an average of the total maximum force over the entire hand and risk insufficient sensitivity at these pressure concentrations, we consider the maximum pressure that can be exerted by a finger over a single phalanx contact pad – the theoretical limit. According to work on tendon arrangements and muscle forces in the human hand [20, 21], the maximum force across a single finger phalanx can reach up to 175N, typically in the thumb or larger fingers and about the proximal phalanx. Approximating the index finger as a compliant cylinder and taking its circumference as 7.3 cm (the mean for males, [22]), we can expect a rectangular contact area of 5.4cm^2. Given the maximum force of 175N exerted by a single finger, we can calculate the range of expected pressures on a single phalanx pad up to 325 kPa (worse case), with a nominal pressure around 100kPa.

C. Human Factors and Anatomical Variation

The dimensions of the human hand phalanges can vary by as much as 11% in length [23] and 14% in circumference [22]. Designing a soft sensor glove using high-strain capacity elastomers (up to 900% strain) ensures that the glove will accommodate these large anatomical variations while providing user comfort (low stress concentrations), but this does not guarantee accurate, repeatable motion and force measurements. A loose fitting glove can cause spatial drift and sensing dead zones, so the glove must fit even the smallest of hands such that the pressure sensors are fixed with respect the finger pad surfaces and that the strain sensors are pre-loaded when the hand is at rest (flat). A snug glove fit can be achieved by selecting the dimensions of the pressure and strain sensors to fit smaller hands and allowing the intrinsic flexibility of the elastomer substrate to accommodate larger hands. Using the experimental characterization of human hand morphology reported in [23], shown in Table II, we set the maximum strain sensor length to the shortest non-distal phalanx, which is 15.57mm, rounded down to 15mm. Assuming that each tensile strain sensor's axial centerline is aligned with the joint axis, this guarantees that there is no overlap between adjacent strain sensors on any phalanx. Because the MCP joints have more space available than the PIP or DIP joints, they may be more prone to axial positioning offsets (sensor not centered over joint). A 25mm strain sensor is also included in the modular sensor suite to allow sufficient strain across the knuckles even with misalignment.

The diameter of the soft pressure sensor was set to 1cm in accordance with the finger circumference data found in [22]. This helps ensure that the pressures recorded by these sensors is due primarily to normal forces, and that these forces can be distributed more evenly across the finger. The width of the strain sensors was set to 1 cm in order to cover the surface of the knuckles without protrusions.

III. SOFT SENSOR DESIGN AND EVALUATION

The designs of the modular soft pressure and strain sensors used in this glove are based on the deformation of liquid-metal channels embedded in elastomer substrates. The geometry of a conductive liquid channel embedded in an elastic body changes when that body is deformed by compression or stretching, changing its electrical resistance. Assuming that the cross-sectional area of the channel and the electrical properties of the conductive liquid are known, changes in channel resistance and, by extension, sensor responses to external forces can be predicted.

TABLE II
PHALANX LENGTH VARIATIONS IN THE HUMAN HAND (mm)

Digit	*Metacarpal*	*Proximal*	*Medial*	*Distal(tissue)*
Thumb	*46.22±3.94*	31.57±3.13	NA	27.34±2.21
Index	*68.12±6.27*	39.78±4.94	22.38±2.51	19.66±2.85
Middle	*64.60±5.38*	44.63±3.81	26.33±3.00	21.35±2.46
Ring	*58.00±5.06*	41.37±3.87	25.65±3.29	21.25±2.82
Little	*53.69±4.36*	32.74±2.77	18.11±2.54	19.69±3.07

The lengths of phalanges, metacarpals and soft tissues of the distal phalanges as reported in [23]. Given these values, maximum dimensions for the pressure and tensile strain sensors were set.

A. Pressure Sensors for Contact Force Measurement

Applying pressure to the surface of a liquid-metal embedded elastomer decreases the cross-sectional area of the channel and increases its resistance, as shown in previous work [15]. The degree of resistance change in the channel is dependent upon the following:

- *Material properties*: Young's modulus, *E,* and Poisson's ratio, *v*, govern static deformation mechanics.
- *Sensor geometry*: elastomer thickness and channel dimensions and topology determine strain sensitivity range and direction. Pressure sensor channel topology is spiral to minimize response to off-axis strains [15].
- *Distribution of external forces*: humans grasp objects of varying size and shape with soft, cylindrical fingers, so non-uniform pressure distributions must be considered.

Assuming a rectangular channel and a uniform applied pressure p, the resistance change can be expressed as

$$\Delta R_p = \frac{\rho L}{wh}\left\{\frac{1}{1-2(1-\upsilon^2)w\chi p / Eh}-1\right\} \quad (1)$$

where w and h are channel width and height, respectively (Fig. 3), and χ is a correction term described in [24] as a function of conductive channel depth, pressure application area, and the offset between the channel and pressure area centerlines. If modeled properly, the conductive liquid channel geometry and spiral-shaped sensor topology can be tuned such that the total range of electrical resistance spans 0-165kPa of expected pressures that deform the channels, providing sufficient sensitivity for the target application.

Several factors limit our ability to vary sensor geometry parameters and tune pressure sensor sensitivity in practice. Glove thickness is limited to less than 2.5mm to maintain a low-profile, leaving no room for variation in h. Previous work [25] established that, with soft sensors fabrication methods available at the time, the minimum channel septum width possible without incidence of septum delamination was 200µm for PDMS and that sensors with surface layers which are thin relative to the channel height had a much higher incidence of "channel pinching" or collapsing, which causes large, temporary resistance increases. To eliminate pinching and delamination and maintain a low device profile, we adhere to previous design guidelines and set w to 300µm and h to 1000µm (half of the sensor height). The remaining design variables are topology and material type.

The relationship between the spiral channel topology its base channel resistance is defined by the pitch d_p of the spiral, the outer diameter d, and the number of turns in it N, which affect the channel length (2). Modeling the spiral sensor as the wrapped linear sensor strip of length L_{spiral}, we estimate the resistivity of the sensor (Fig.3) and compare to compressive strain test data (Fig. 4)

$$L_{spiral} = \sqrt{(\pi dN)^2 + (d_p N)^2} \quad (2)$$

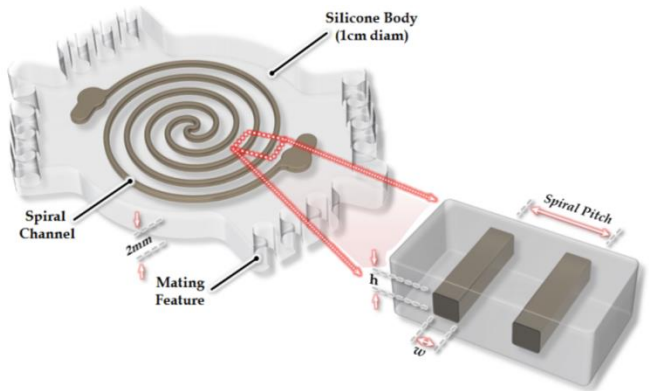

Fig. 3. Model of the pressure sensor. Though the channel is spiral in shape, the resistance changes can be approximated by modeling the spiral as a coiled rectangular strip in (1).

Compressive tests were done on an Instron 5540 Series mechanical testing system (Instron Inc., USA). Pressure was ramped to 110kPa (17.25N applied with a 1cm diameter contact plate) using a triangular loading profile over 10 cycles. Results show high sensor response repeatability, hysteresis (expected), and a mismatch with predictions at high pressures, likely due to modeling assumptions.

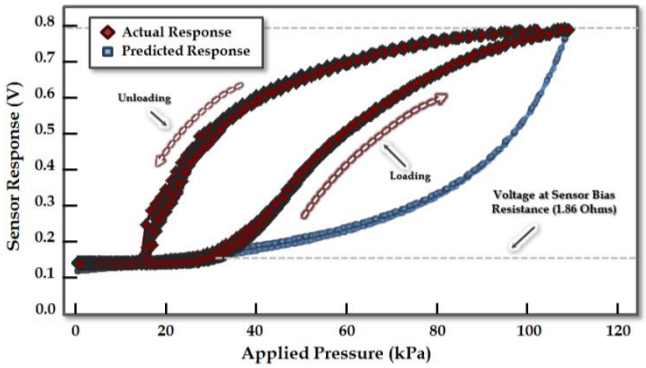

Fig. 4. Response of a pressure sensor 1cm in diameter and 2mm in thickness with h = 500µm, w = 300µm, and L = 157.4mm. Resistance changes were recorded using a voltage divider with a 1V source and 10 Ohm reference.

B. Strain Sensors for Joint Motion Measurement

Applying a tensile force along a conductive liquid channel produces axial strains which serve to increase the length of the channel and decrease the cross-sectional area, increasing the total channel resistance [15] (Fig 5). The relationship between resistance change and strain is given by

$$\Delta R_{ext} = \frac{\rho L}{wh}\left\{\frac{(1+2\nu)\varepsilon - \nu^2\varepsilon^2}{(1-\nu\varepsilon)^2}\right\}. \quad (3)$$

The strain sensor sensitivity is tuned by adjusting channel width and height, w and h. Channel cross-section dimensions are held constant to accommodate design constraints, so sensitivity is modified only by increasing channel length along the sensor's strain axis or by increasing the number of channel segments. This design uses four channel segments, the maximum allowed by dimension and process constraints.

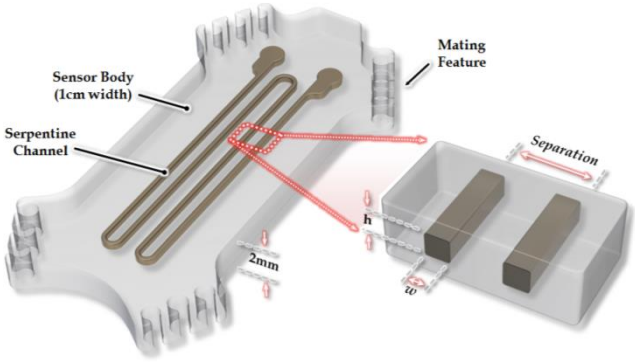

Fig. 5. Model of the strain sensor. Though the sensor channel is serpentine in shape and does not adhere to assumptions made in (1), the total resistance change per unit strain can be approximated by modeling the serpentine path as a folded rectangular strip.

Bench top measurements show that patches of skin 1cm distal and 1cm proximal to interphalangeal joints stretch up to 29% over the joint's motion range. The force required to cause this much strain in these soft tensile strain sensors ($E \approx$ 30 kPa [26]) is negligible (~0.6N) compared to forces produced during normal hand motions (50N+).

Figure 6 shows the response of the strain sensor under both tensile loading and off-axis normal loading. Sensitivity to tensile loads, applied by extending the sensor 20mm/min over 10 cycles, was high. Sensitivity to off-axis normal loads was relatively low. Though the normal loads only reached 1N here (as opposed to the 17.5N used for pressure sensors), we would expect loads on the back of the finger to be this low given the strength of the extension muscles [21].

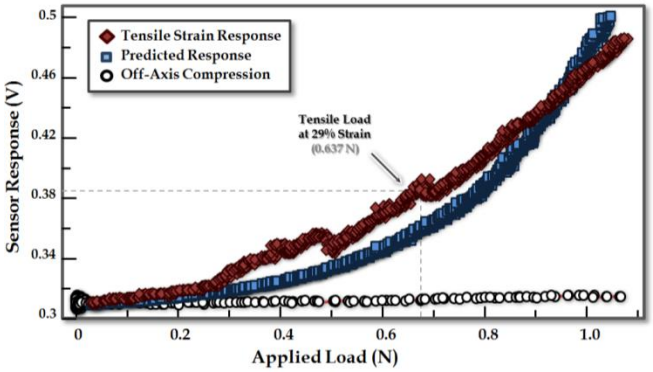

Fig. 6. Response of a strain sensor 1cm in width and 2mm in thickness with a h = 500µm, w = 300µm, and L = 97mm. Resistance changes were recorded using a voltage divider with a 1V source and 10 Ohm reference.

C. Glove Design and Sensor Network Topology

This work focuses on proving the concept of a multimodal soft sensing glove in the form of a single digit soft data glove. This soft "finger glove" (Fig. 7) addresses many of the sensor design, fabrication, and assembly challenges involved in creating a full hand glove, but the scale of the finger glove has allowed for more design iterations and experiment validations than possible otherwise. One question which remains for a full hand glove implementation is the coupling of sensing between neighboring fingers, but we anticipate addressing this in future work.

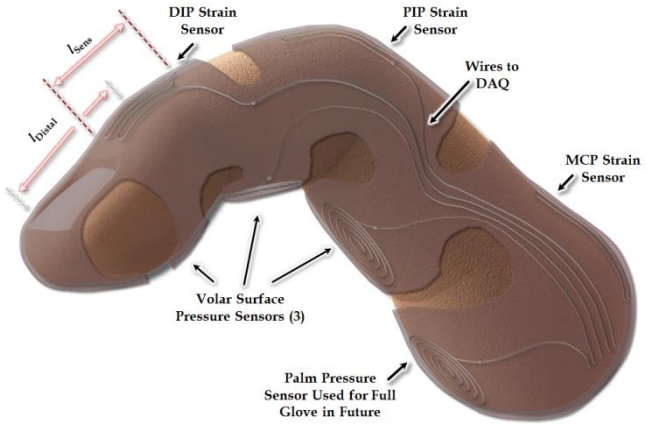

Fig. 7. Model of a soft finger glove (index finger) with integrated pressure and strain sensors. The length of the strain sensors is less than half the length of the proximal phalanx of the target joint, as design rules specify.

The finger glove contains three tensile strain sensors used to measure the individual joint motions, and three pressure sensors which are used to capture interaction dynamics on the volar surface of the hand during object manipulation (Fig. 7). The sensors are fabricated as modular units that are later assembled in a network to create the soft finger glove.

IV. Fabrication

Key contributions of this work are the process innovations which enable the assembly of complex soft sensor networks from such modular sensors. Modular fabrication has a higher production yield than monolithic approaches as faulty sensors can be rejected before inclusion into a sensor network or replaced in a network after a failure. This section describes the fabrication and assembly process.

A. Individual Sensor Fabrication

Sensors for the soft finger glove prototype were fabricated used a layered molding and casting process. This process can be divided into four steps: 1) functional component embedding (Fig. 8), 2) silicone casting, 3) layer bonding, and 4) conductive liquid injection. The details of this process can be found in [15,16,24,25]. The base material for the sensors is the silicone rubber EcoFlex (Smooth-On Inc., Easton, PA, 18042, USA), a two-part elastomer capable of high strains (900% at failure). The conductive liquid used is a eutectic alloy of gallium-indium-tin, or "gallinstan" (Ga:In:Sn; 62:22:16 wt%; from AlfaAesar, Ward Hill, MA, USA). The completed sensors are shown in Fig. 9.

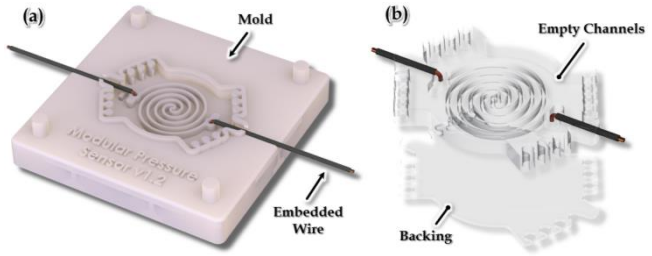

Fig. 8. Soft sensor fabrication process innovations in this work include (a) placement of embedded sensor components into mold before (b) silicone casting and curing.

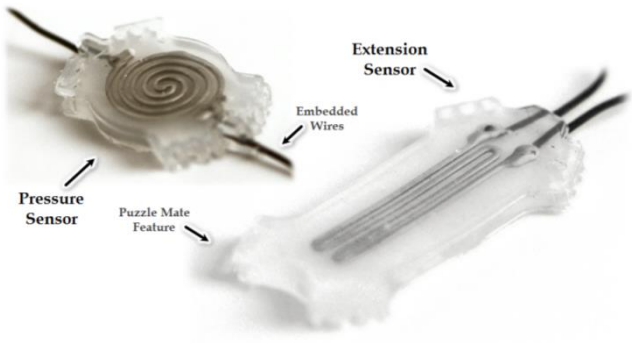

Fig. 9. Photos of fabricated soft strain and pressure sensors, both with mating features and embedded wires.

B. Sensor Integration Features

The assembly of the sensor glove's sensor network requires secure cohesive bonds between several individual, pre-cured elastomer bodies of similar chemical composition. The strength of these cohesive bonds depends on several parameters including degree of chemical surface activation, atmospheric moisture, and mating surface shape and cleanliness. In a well-conditioned and controlled fabrication environment and with surface activation – a benefit to bond strength – being low after a full cure, the cohesive bonds are affected primarily by the mating surface shape. Inspired in part by previous work, which uses silicone rubber to achieve strong mechanical bonds in shape deposition manufacturing [27], we investigated the use of three different surface features as our mechanical mating method (Fig. 10):

- *Flat Surfaces*: smooth sensor mating surface with no special mating features or embedded components.
- *Puzzle Surfaces*: a serpentine surface profile which increases the total mating surface area by over 300%.

Embedded Strain Supports: a flexible laser-patterned strain support which allows silicone columns to form within its structure, providing a mechanical anchor.Each sensor mating surface type was cast into molds with 1cm x 2mm rectangular cross sections. Five samples of each mate surface type were fabricated for a total of 15. These samples were fully cured, along with five monolithic samples and placed into molds with space to cast another strip of silicone rubber onto the cured mating surface. After casting the second strip, the samples were fully cured.

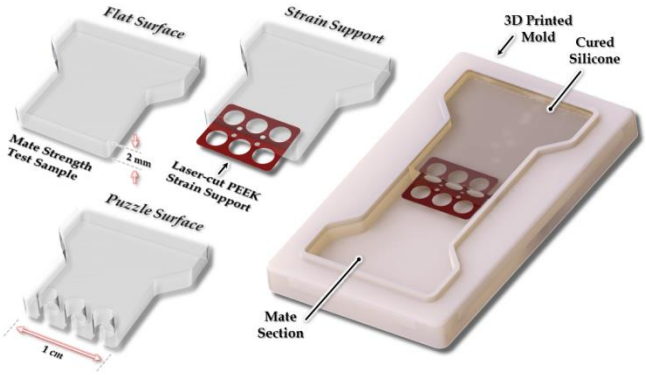

Fig. 10. Samples of the three mate types – flat, puzzle, and strain support- used in the interface mate strength characterization experiment.

The cured test samples were clamped using pneumatic vices onto an Instron 5540 Series electro-mechanical testing system (Instron Inc., USA) where they were loaded in tension until failure. The resulting data demonstrated that the puzzle interface provided the best, most consistent bond strength for a minimal change in fabrication process (no additional steps; supports add three steps). The puzzle mate interface was subsequently chosen as the preferred mechanical integration method for the glove (Fig. 11).

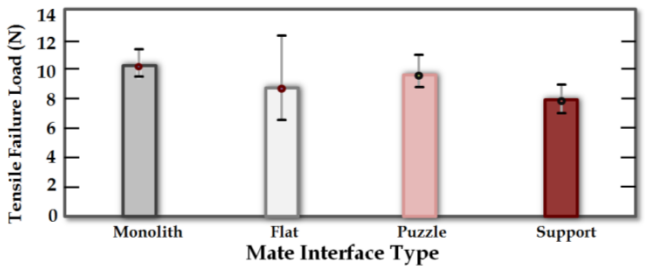

Fig. 11. Mate interface strength testing indicated that the puzzle interface strength is comparable to monolithic structures after a full cure. Error bars show the measurement extremes of samples tested for each mate interface.

C. Glove Molding

Assembling the modular soft sensors into a glove-based sensor network requires an encapsulation molding process. The encapsulation mold (Fig. 12) provides a template for the spatial layout of the modular sensors during encapsulation pours. The modular sensors are placed in the mold and EcoFlex in poured around them in a glove pattern to complete the device (shown being worn in Fig. 13).

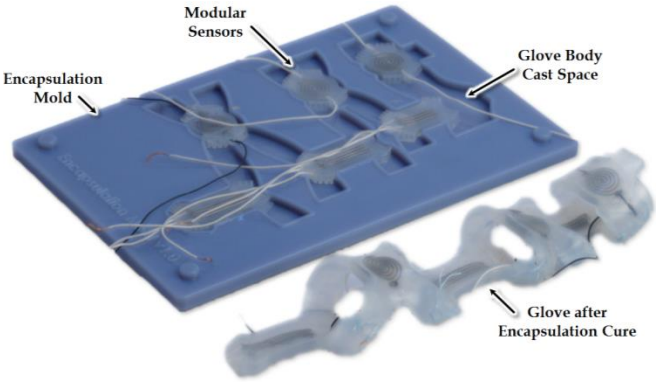

Fig. 12. A photo of the soft sensor encapsulation with strain and pressure sensor inserted and the soft finger glove after mold release and fastening.

V. Experimental Validation

The soft finger glove was experimentally validated through manipulation experiments in which the user grasped daily living objects (Fig. 14) and the glove simultaneously measured both tactile pressures and joint motion.

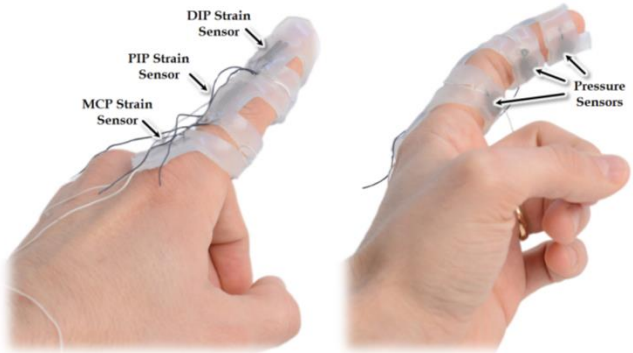

Fig. 13. A photo of the completed soft sensor finger glove worn by a user. The glove is pictured untethered here for visualization purposes.

A. Sensor Calibration and Repeatability Test

Calibration of the pressure sensors was done by measuring the bias voltage of each sensor - with no external pressure applied - via a voltage divider having a 1V source and 10Ohm reference resistance, then measuring the sensor under a known applied load (electromechanical tester). The strain sensors are calibrated by precisely positioning each joint using acrylic finger constraints [28] and measuring the resistance at each angle (0˚,45˚,90˚).

B. Hand Gesture and Object Grasping Tasks

The ability to measure joint motions and tactile pressures with the soft finger glove (index finger) is tested by grasping three daily living objects: a coffee mug (513.5g), a hammer (450.0g), and a textbook (578.2g). After the glove user acquired a stable grasp of the objects, the voltages across the strain and pressure sensors were recorded and the pressure and strain values were calculated according the calibration values and (1) and (3). This was done over several trials as a proof of concept. Representative data is furnished here. Ground-truth measurements were not taken to verify actual angles during grasping but future work will include this data.

Fig. 14. The soft finger glove being worn while grasping test objects.

VI. Results and Discussion

A. Evaluation of Glove Performance

Experimental data demonstrates the sensitivity of the soft pressure and strain sensors in finger glove to the range of pressures (0-165kPa) and tensile strains (30%) required to measure full anthropomorphic hand motions and interaction pressures during every day human grasping (Section III) and the ability to measure both quantities simultaneously. Figure 15 shows the difference in finger postures for grasps acquired on the three objects. The textbook grasp has the smallest measured flexion angles, as expected for flat objects, while the hammer grasp had large flexion angles associated with power grasps of cylindrical objects.

Figure 16 illustrates the difference in tactile pressures distributed across the index finger during grasping. The hammer required the highest pressures by far (large mass and momentum during use), while the textbook and coffee mug grasps had relatively small tactile pressures. These tactile pressure profiles – important data for human grasp mechanics and robot hand design research - are not attainable using many of the current sensor glove solutions.

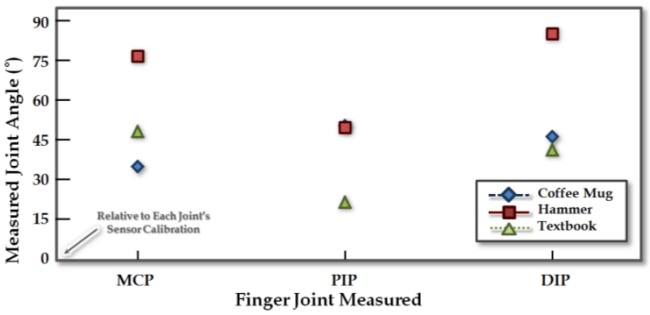

Fig. 15. Joint angles recorded during grasping of daily living objects (one grasp per object), calculated from tensile strain sensor responses.

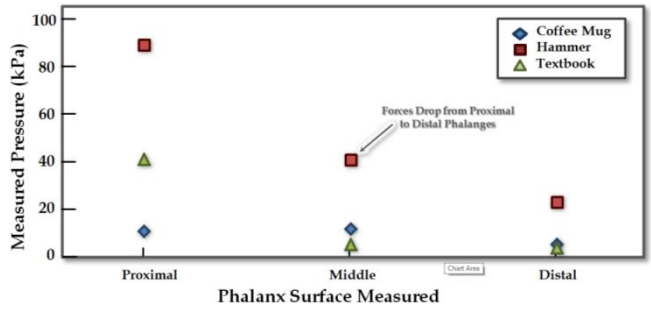

Fig. 16. Tactile pressures recorded during grasping of daily living objects and calculated from pressure sensor responses.

Figure 17 demonstrates sensitivity to both static grasp motion/pressures but also low-frequency dynamics associated with object utilization (at the proximal sensor). The progression of the hammer grasp, including initial grasp acquisition, grasp correction to acquire a stronger grasp, and subsequent pressure fluctuations during hammer use, is seen.

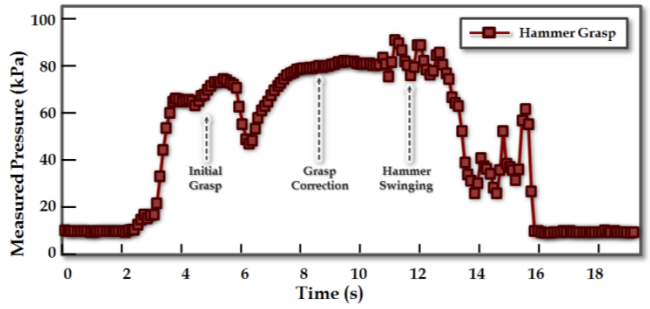

Fig. 17. Temporal profile of tactile pressures on the proximal phalanx during hammer swinging. Grasp force increases after grasp correction.

B. Mechanical Robustness

Despite promising results, we also encountered a few technical issues including the thickness of the glove sensors (2mm) its effect on grasp acquisition and quality, the failure of pressure sensors under high loads by septum delamination and leaking near embedded wires (40% of tested sensors), and the off-axis, in-plane preloading of sensors during glove donning which could affect bias resistance and non-linear sensing ranges. These can be remedied in part by refining the fabrication process and embedding strain relief supports. The use of rigid wires in the soft glove did not pose mechanical robustness issues as wires were located away from primary loading/deformation sites.

VII. Conclusion and Future Work

This initial work toward a modular, low-cost soft sensor-embedded glove demonstrates the efficacy of novel soft sensor design and assembly methods we developed to enable sophisticated, soft sensor-embedded wearable devices requiring networks of these sensors.

In this paper, we designed soft sensors to measure contact pressures and strains within a range specific to human grasping and gesturing, and we validated these sensitivity ranges using electromechanical testing equipment. We developed a novel soft fabrication method which enables the embedding of wires during the sensor fabrication to significantly increase sensor production yield. We also developed a mechanical integration method which allows fast, reliable assembly of several individually manufactured and tested soft sensors into large sensor networks, allowing efficient fabrication of complicated devices like the soft data glove with high manufacturing efficiency. We used the optimized strain and pressure sensors, along with our fabrication process innovations, to create a soft finger glove. We experimentally evaluated the glove's ability to provide accurate grasp motion and force data (static and dynamic) by having human subjects grasp and use a variety of objects.

Future work will focus on refining the manufacturing process to address challenges with conductive liquid injection and redesigning pressure sensors to prevent septa delamination seen during high-force tasks. Work will also be done to compute a gain matrix to account for kinematic coupling between sensor DOFs, explore the role of object shape and stiffness on the accuracy and response of the pressure sensors, investigate the effect of shear forces on sensor performance, design a sensor-embedded palm and inter-digital (IDA) separation sensors, and integrate the palm and finger gloves to create a full-hand sensor glove.

Acknowledgment

The authors gratefully acknowledge the Wyss Institute for Biologically Inspired Engineering for supporting this work. Opinions, findings, and conclusions or recommendations expressed in this material are those of the authors and do not necessarily reflect the views of the Wyss Institute.

References

[1] D. Bowman, C. Wingrave, J. Campbell, and V. Ly, "Using Pinch Gloves(TM) for both Natural and Abstract Interaction Techniques in Virtual Environments". *Tech. Report TR-01-23*, Virginia Tech, 2001.

[2] G. Saggio, F. Giannini, M. Todisco, and G. Costantini. "A data glove based sensor interface to expressively control musical processes," *4th IEEE International Workshop on Advances in Sensors and Interfaces*, Savelletri di Fasano, Italy, 2011, pp. 192-195.

[3] J. Connolly, K. Curran, J. Condell, and P. Gardiner, (2011, May). "Wearable rehab technology for automatic measurement of patients with arthritis," *IEEE Pervasive Computing Technologies for Healthcare*, Dublin, Ireland, 2011, pp. 508-509.

[4] L. Dipietro, A. Sabatini, P. Dario, "A Survey of Glove-Based Systems and Their Applications," *IEEE Trans. on Sys, Man, and Cybernetics-Part : Applications and Reviews,* vol. 38, no. 4, pp. 461-481, 2008.

[5] D. J. Sturman and D. Zeltzer. "A survey of glove-based input," *IEEE Computer Graphics and Applications*, vol. 14, no. 1, pp. 30-39, 1994.

[6] K. N. Tarchanidis, J. N. Lygouras, "Data glove with a force sensor," *IEEE Trans. on Instrumentation and Measurement*, vol. 52, no. 3, pp. 984-989, 2003.

[7] J. L. Hernandez-Rebollar, N. Kyriakopoulos, and R.W. Lindeman, "The AcceleGlove: A whole-hand input device for virtual reality," *Proc. SIGGRAPH*, 2002, pp. 259.

[8] J. H. Kim, N. D. Thang, amd T. S.Kim, "3-D hand motion tracking and gesture recognition using a data glove," *IEEE Int. Symposium on Industrial Electronics*, 2009, pp. 1013-1018.

[9] Y. Han,. "A low-cost visual motion data glove as an input device to interpret human hand gestures." *IEEE Transactions on Consumer Electronics*, vol. 56, no. 2, pp. 501-509. 2010.

[10] B. Howard and S. Howard, "Lightglove: Wrist-worn virtual typing and pointing," in *Proc. IEEE Int. Symp. Wearable Comput*., Zurich, Switzerland, 2001, pp. 172–173.

[11] N. Tongrod, T. Kerdcharoen, N. Watthanawisuth, and A. Tuantranont. "A low-cost data-glove for Human computer interaction based on ink-jet printed sensors and ZigBee networks." *IEEE Int. Symp. on Wearable Computers*, Seoul, South Korea, 2010. pp. 1-2.

[12] A. Tognetti, N. Carbonaro, G. Zupone, and D. De Rossi, "Characterization of a novel data glove based on textile integrated sensors," *28th Annual Int. Conf. of the IEEE Engineering in Medicine and Biology Society*, New York, NY, USA 2006, pp. 2510-2513.

[13] R. Kramer, C. Majidi, and R.J. Wood," Wearable Tactile Keypad with Stretchable Artificial Skin," in *Proc. IEEE Int. Conf. on Robotics and* Automation, Shanghai, China, 2011, pp. 1103-1107.

[14] S. J. Leigh, R. J. Bradley, C. P. Purssell, D. R. Billson, D. A. Hutchins, "A Simple, Low-Cost Conductive Composite Material for 3D Printing of Electronic Sensors," *PLoS ONE*, vol. 7. no. 11, 2012, e49365. doi:10.1371/journal.pone.0049365.

[15] Y. L. Park, B. Chen, R. J. Wood, "Design and Fabrication of Soft Artificial Skin using Embedded Microchannels and Liquid Conductors," *IEEE Sensors J.*, vol. 12, no. 8, pp. 2711–2718, 2011.

[16] Y. Menguc, Y. L. Park, E. Martinez-Villalpando, P. Aubin, M. Zisook, L. Stirling, and C. J. Walsh, "Soft wearable motion sensing suit for lower limb biomechanics measurements," *IEEE Int. Conf. on Robotics and Automation*, Tokyo, Japan, 2013, pp. 5309-5316.

[17] S. Cobos, M. Ferre, S. Uran, J. Ortego, and C. Pena, "Efficient human hand kinematics for manipulation tasks,' *IEEE/RSJ International Conference on Intelligent Robots and System*s. Nice, France, 2008, pp. 2246-2251.

[18] M. C. Hume, H. Gellman, H. McKellop, and R. H. Brumfield Jr., "Functional range of motion of the joints of the hand," *The Journal of Hand Surgery*, vol. 15, no. 2, pp. 240-243, 1990.

[19] V. Mathiowetz, N. Kashman, G. Volland, K. Weber, M. Dowe, and S. Rogers, "Grip and pinch strength: normative data for adults," *Archives of physical medicine and rehabilitation*, vol. 66, pp. 69-74, 1985.

[20] K. An, E. Chao. W. Cooney, and R. Linscheid, "Forces in the Normal and Abnormal Hand," *J. Orthopaedic Res.*, vol. 3 pp. 202-211, 1985.

[21] N. Pollard and D. Gilbert, "Tendon Arrangement and Muscle Force Requirements Force Capabilities in a Robotic Finger," *IEEE Int. Conf. of Robotics and Automation*, Washington, DC, 2002, pp. 3755-3762.

[22] C. F. Bolton and K. C. Carter, "Human sensory nerve compound action potential amplitude: variation with sex and finger circumference," *Journal of Neurology, Neurosurgery, and Psychiatry*, vol. 43, pp. 925-928, 1980.

[23] B. Alexander and K. Viktor, "Proportions of Hand Segments Int. *J. of Morphology*, vol. 28, no. 3, pp. 755-758, 2010.

[24] Y. L. Park, C. Majidi, R. Kramer, P. Berard, R. J. Wood, "Hyperelastic Pressure Sensing with a Liquid-Embedded Elastomer," *Journal of Micromechanics and Microengineering*, vol. 20, 2010.

[25] F. Hammond III, Q. Wan, R. Kramer, R. Howe, and R. Wood. "Soft Tactile Sensor Arrays for Force Feedback in Micromanipulation," *IEEE Sensors Journal*, to be published.

[26] P. Boonvisut, R. Jackson, and M. C. Cavusoglu. "Estimation of soft tissue mechanical parameters from robotic manipulation data." *IEEE Int. Conf. Robotics and Automat.,* St. Paul, MN, pp. 4667-4674, 2012.

[27] A. M. Dollar, C. R. Wagner, and R. D. Howe, "Embedded sensors for biomimetic robotics via shape deposition manufacturing*," IEEE/RAS-EMBS Int. Conf. in Biomedical Robotics and Biomechatronics*, Pisa, Italy, 2006, pp. 763-768.

[28] G. D. Kessler, L. F. Hodges, and N. Walker. "Evaluation of the CyberGlove as a whole-hand input device." *ACM Transactions on Computer-Human Interaction,* vol. 2, no. 4 pp. 263-283, 1995.